JOURNAL OF combinatorial CHEMISTRY

Article

Synthesis of Electroconducting Narrowly Distributed Nanoparticles and Nanocomposite Films of Orthanilic Acid/Aniline Copolymers

Xin-Gui Li, Rui-Rui Zhang, and Mei-Rong Huang

J. Comb. Chem., **2006**, 8 (2), 174-183• DOI: 10.1021/cc050126y • Publication Date (Web): 01 February 2006

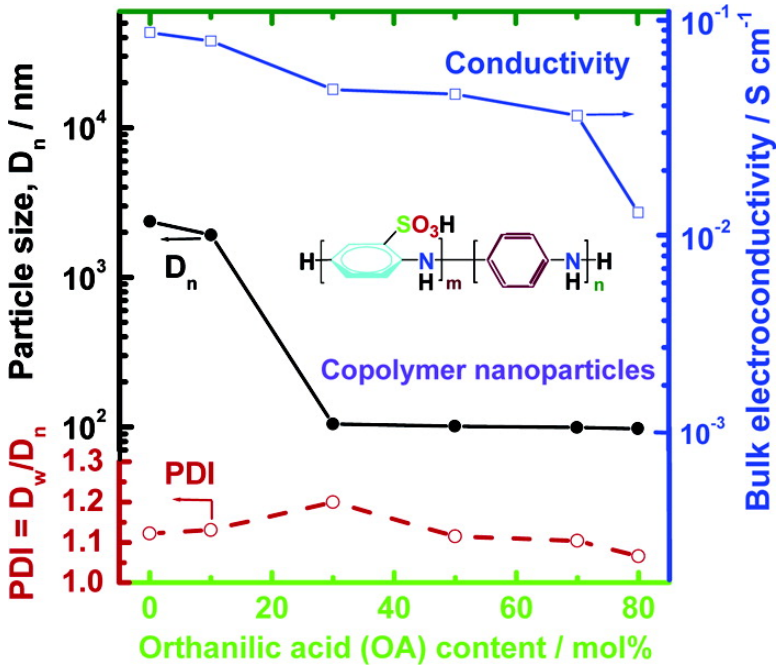

More About This Article

Additional resources and features associated with this article are available within the HTML version:

- Supporting Information
- Links to the 2 articles that cite this article, as of the time of this article download
- Access to high resolution figures
- Links to articles and content related to this article
- Copyright permission to reproduce figures and/or text from this article

View the Full Text HTML

Journal of Combinatorial Chemistry is published by the American Chemical Society.
1155 Sixteenth Street N.W., Washington, DC 20036

Synthesis of Electroconducting Narrowly Distributed Nanoparticles and Nanocomposite Films of Orthanilic Acid/Aniline Copolymers

Xin-Gui Li,*,†,‡ Rui-Rui Zhang,† and Mei-Rong Huang†

Institute of Materials Chemistry, Key Laboratory of Advanced Civil Engineering Materials, School of Materials Science and Engineering, Tongji University, 1239 Siping Road, Shanghai 200092, China, and Department of Chemistry, The Shanghai Key Laboratory of Molecular Catalysis and Innovative Materials, Fudan University, Shanghai 200433, China

Received September 23, 2005

A unique strategy for synthesis of narrowly distributed and inherently self-stabilized copolymer nanoparticles by a simple emulsifier-free polymerization from orthanilic acid and aniline was developed. The polymerization yield, electrical conductivity, size, and its distribution of the nanoparticles could be simultaneously optimized by facilely regulating the comonomer ratio, oxidant/comonomer ratio, polymerization temperature, and time. In particular, the nanoparticles evermore exhibit a size polydispersity index down to 1.066 and strong redispersibility in water or polymer solutions. This facile synthesis of functional nanoparticles using orthanilic acid as vital comonomer readily affords yields up to 80%. A low percolation threshold of the nanoparticles/cellulose diacetate and poly(vinyl alcohol) nanocomposite films was found to be 0.18 and 0.07 wt %, respectively. This study opens a simple and general route for fabrication of nanostructured polymer materials with controllable size, narrow size distribution, intrinsic self-stability, strong dispersibility, high purity, and regulable electroconductivity.

Introduction

Sulfonated polyaniline (SPAN) is the focus of polyaniline (PAN) derivatives in view of its unique electroactive physical properties, easy processability, and wide variety of potential industrial applications, including secondary rechargeable batteries,[1] sensors,[2,3] electrochromic materials,[4] light-emitting diode devices,[5] and corrosion protection.[6] SPAN can compare favorably with PAN because SPAN contains an ionizable, negatively charged functional group,[7] which acts as an inner dopant anion and also stabilizer, bound to the polymer backbone. Thus, no anion exchange between the SPAN and surroundings takes place during the redox process. The charge compensation originates from moieties covalently bound to the polymer at the expense of a proton exchange, which occurs much faster and does not limit the redox speed.

A variety of synthetic routes have been developed to achieve a controlled synthesis of SPANs.[8,9] In contrast to electropolymerization,[10] chemical oxidative polymerization overcomes the restriction by electrode area for successful application of the conducting polymer. It is noteworthy that the SPAN prepared by the copolymerization method seems to be more thermally stable than the SPAN of the same degree of sulfonation prepared by the postsulfonation method. This phenomenon has been explained by the higher steric strain in postsulfonated SPAN chains, leading to their distortion and lower thermodynamic stability.[11] Another important predominance of copolymerization of substituted aniline (AN) with AN is that it can afford a polymer with novel morphology and properties.[9] Furthermore, the sulfonic groups on the chains could be efficiently served as an internal stabilizer, owing to their interchain electrostatic repulsion, thus leading to an in situ fabrication of the fine nanoparticles in the absence of any external stabilizers.[12,13] The synthesis of these external stabilizer-free nanoparticles can successfully prevent a relatively complicated preparation in dispersion polymerization[14] and low purity in microemulsion polymerization.[15] The synthesis of functional nanoparticles with a self-stability and narrow size distribution is receiving the attention of scientists interested in developing advanced nanomaterials and -devices. To realize this objective, orthanilic acid (OA) and AN were carefully chosen to facilely synthesize pure nanoparticles with intrinsically electrical conductivity and magnetism.[16] Until now, no studies have been reported on the synthesis of the OA/AN copolymer nanoparticles.

Here, we reported a direct preparation and characterization of OA/AN copolymer nanoparticles having a narrow size distribution by a simple single-step, emulsifier-free polymerization that is much more convenient than traditionally multistep dispersion or emulsion polymerization. The effect of important polymerization parameters, including the OA/AN ratio and polymerization conditions on the polymerization yield, structure, and properties of the nanoparticles has been systematically investigated. The evidence for the formation of the spheroidal nanoparticles is elaborated, and the unique formation mechanism for the pure nanoparticles is proposed. In addition, the nanoparticles were successfully applied to fabricate conductive nanocomposite films with an

* To whom correspondence should be addressed. E-mail: adamxgli@yahoo.com.
† Tongji University.
‡ Fudan University.

10.1021/cc050126y CCC: $33.50
Published on Web 02/01/2006

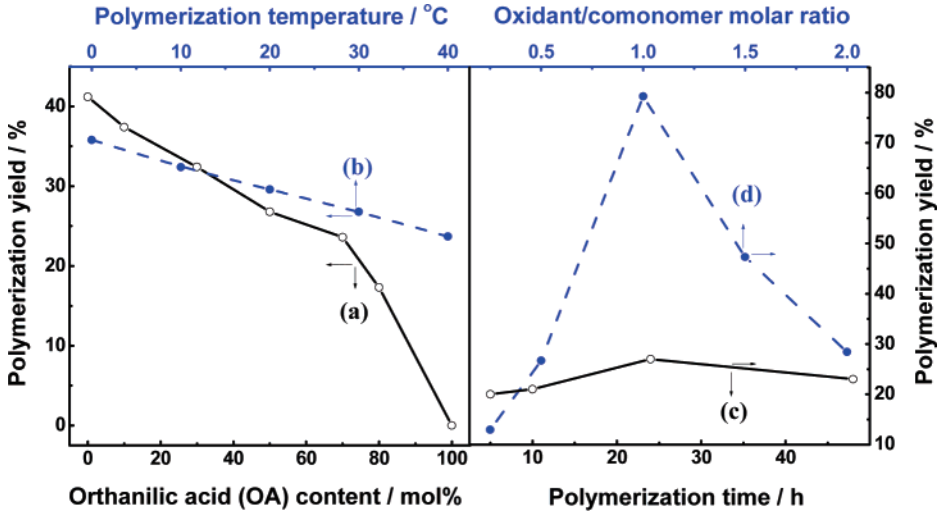

Figure 1. Effects of comonomer ratio and polymerization conditions on the OA/AN polymerization yield. Polymerization conditions: (a) oxidant [$(NH_4)_2S_2O_8$]/monomer molar ratio of 0.5/1 for a polymerization time of 24 h at a polymerization temperature of 30 °C; (b) OA/AN molar ratio of 50/50 with an oxidant [$(NH_4)_2S_2O_8$]/monomer molar ratio of 0.5/1 for a polymerization time of 24 h; (c) OA/AN molar ratio of 50/50 with oxidant [$(NH_4)_2S_2O_8$]/monomer molar ratio of 0.5/1 at 30 °C; (d) OA/AN molar ratio of 50/50 for polymerization time of 24 h at 30 °C.

extremely low percolation threshold but high transparency. This methodology facilitates the systematic study of the relationship between the nanoparticle formation and polymerization condition. The new system offers the possibility of changing several parameters of a polymerization recipe, for example, in terms of OA/AN ratio, oxidant/comonomer ratio, polymerization temperature, and time but with constant vessel, stirrer geometry, and agitation rate. This investigation may promote the optimization of the polymerization conditions (comonomer ratio, oxidant/comonomer ratio, temperature, and time) for the facile and reproducible synthesis of the nanoparticles at high yield and electroconductivity.

Results and Discussion

Synthesis of the OA/AN Copolymer Particles. In the OA/AN copolymerization process, the potential experienced a sudden increase first; then a dramatic decrease; and finally, kept almost constant until the end of the polymerization. The polymerization time corresponding to the maximum potential became longer with increasing OA content. This phenomenon illustrates that the polymerization rate significantly reduces with introduced OA comonomer, implying a prolongation of the chain initiation and propagation periods. The maximum potential shows a minimum at an OA content of 10 mol %. That is to say, the maximum potential of the copolymerization solution is not a simple addition of the potentials of the homopolymerization solutions of two comonomers. It is coincident that the solution temperature of all comonomer ratios reaches the maximum value at the maximum potential, indicating the maximal rate point of molecular chain propagation. It is seen that the addition of oxidant makes the reaction mixture turn dark violet, signifying the occurrence of oxidative polymerization. With increasing OA amount, it takes a longer time for polymer particle precipitation to occur and for the solution color to turn claret. These phenomena validate a close relationship between protonation and maximum potential during oxidative polymerization because the protonation is the first step of oxidative polymerization. This behavior coincides with the reactivity ratio of AN (2.99), which is much higher than that of OA (0.06),[16] exhibiting electron-withdrawing and steric hindrances effects from $-SO_3H$.

The effect of four polymerization conditions on the OA/AN copolymerization yield is shown in Figure 1. Apparently, the yield steadily decreases with increasing OA content in Figure 1a because of the easy termination of growing chains containing the relatively inert OA monomer unit. Furthermore, it seems that no OA oxidative homopolymer could be obtained, signifying that the OA monomer does not have oxidative homopolymerizability. A slow and linear decrease of the yield with increasing polymerization temperature is found in Figure 1b, because low temperature is favorable for the growing of the polymer chain containing more AN repeating units with AN monomers. A similar relationship between the yield and temperature has been observed for the *p*-phenylenediamine/*o*-phenetidine copolymerization.[17] It is interesting that the polymerization yield exhibits a maximum with changing polymerization time and oxidant/comonomer ratio, which is also something like the situation of the *p*-phenylenediamine/*o*-phenetidine copolymerization.[17] The optimal polymerization time for the highest polymerization yield is ~24 h, since too long a time could lead to apparent hydrolysis of as-formed polymers in the acidic medium.[17] An increasing oxidant/monomer ratio produces a much higher yield, because more oxidant provides many more initiators in the polymerization system, and yet excessive oxidant would overoxidize or even break up the polymer chains to some extent. The optimum oxidant/monomer molar ratio for the highest polymerization yield is 1. Almost the same relationship between the yield and oxidant/monomer ratio was found for the 3-aminobenzenesulfonic/AN copolymerization.[11] In conclusion, the effect of the polymerization conditions on the yield could rank in a reduced order:

oxidant/comonomer ratio > OA/AN ratio >
polymerization temperature > polymerization time

Molecular Structure of the OA/AN Copolymer Particles. IR spectra for solid OA/AN copolymers illustrate that the intensity ratio of quinoid (1570 cm^{-1}) over benzenoid (1490 cm^{-1}) peaks increases first and then decreases as the OA content rises from 0 to 80 mol %. That is to say, the molecular structure of the copolymers varies nonmonotonically with OA/AN ratio. It appears that OA/AN(50/50) copolymer exhibits the maximal intensity ratio of quinoid over benzenoid peaks, indicating its highest quinoid content. A strong peak at 1305 cm^{-1} should be due to the C−N stretching mode of the quinoid ring. A medium peak at 1242 cm^{-1} may be ascribed to the C−N stretching vibration in benzenoid units. Two absorptions at 1055 and 1002 cm^{-1} are associated with the asymmetric and symmetric O═S═O stretching vibrations of the $-SO_3H$ group, respectively. The peaks at 702 and 607 cm^{-1} are assigned to the characteristic S−O and C−S stretching vibrations, respectively. The four peaks due to the SO_3 group could be used to estimate the OA unit content in the copolymers because their intensity rises steadily with an increase in the OA content. The C−H out-of-plane bending vibration corresponding to the 1,4-substituted benzene rings at 810 cm^{-1} indicates that the OA/AN copolymers have head-to-tail coupling of the OA and AN units, which is analogous to the generally proposed structure of PAN. All the results prove that the OA/AN copolymers have been successfully prepared.

The UV−vis absorption spectra of the OA/AN copolymer solutions with different comonomer ratios exhibit the characteristics of two absorption bands centered at 335 and 620 nm, as listed in Table 1. The strong band at ∼335 nm is due to $\pi-\pi^*$ transition, which corresponds to the band gap, and the broad band around 620 nm is assigned to the $n-\pi^*$ excitation band or interband charge transfer associated with the excitation of benzenoid to quinoid rings. The $\pi-\pi^*$ transition band for the OA/AN copolymers shows a monotonic hypsochromic shift from 336 to 332 nm with increasing OA content from 0 to 80 mol %. It is interesting that the $n-\pi^*$ excitation band wavelength increases first and then decreases with increasing OA content from 0 to 80 mol %. The area ratio of bands II over I also increases first and then decreases. That is to say, the OA/AN(10/90) copolymer exhibits the highest oxidation degree,[18] the longest wavelength of the band II, and the maximal area ratio of band II over I, signifying its longest conjugation length and largest extent of the π-conjugation structure. This should be important evidence of formation of a genuine OA/AN copolymer. Generally, increasing OA content in the polymer would shorten the conjugation length to some extent because the steric and electron withdrawing effects of $-SO_3H$ substituent could produce torsional main-chain and lower electron density on the main chain.

Size and Morphology of the OA/AN Copolymer Particles. Generally, an external stabilizer is considered to be indispensable to the formation and stabilization of the nanoparticles of electrically conducting polymers by a polymerization method. However, the AN derivative units with negatively charged sulfonic groups exhibiting static repulsion that was present on the surface of the as-formed particulates could contribute to the stabilized existence of the resultant nanoparticles.[12,13,19] In other words, the nanoparticles obtained thus are self-stabilized, and their composition is relatively pure because the contamination from external stabilizer, emulsifier, or dispersant is totally prevented. Furthermore, the size of the particles could be controlled by easily regulating the sulfonic group content and synthetic conditions.

Table 1. UV−Vis Spectra of OA/AN Copolymers at a Concentration of 10 mg/dL NMP with Different Comonomer Molar Ratios[a]

OA/AN molar ratio	band I, A (4 eV)		band II, A (2 eV)		area ratio of band II/I
	wavelength (nm)	area	wavelength (nm)	area	
0/100	336	71.0	625	69.2	0.97
10/90	335	67.3	627	71.0	1.05
30/70	335	51.6	625	52.5	1.02
50/50	333	65.1	619	60.0	0.92
70/30	333	92.4	616	72.7	0.79
80/20	332	122.1	614	79.5	0.65

[a] Obtained under the following polymerization conditions: oxidant $[(NH_4)_2S_2O_8]$/monomer molar ratio 0.5/1, polymerization time of 24 h, polymerization temperature of 30 °C, 1.0 M HCl aqueous solution, and by dropping the oxidant solution into the monomer solution.

The OA/AN copolymerization generally affords ultrafine precipitates as products. The stability and size of the particles depend significantly on the sulfonic content in the polymer chains. The number-average diameter (D_n) and polydispersity index (PDI, defined as D_w/D_n, where D_w means weight-average diameter) of the OA/AN copolymer particles in water are systematically shown in Figure 2. The D_n first decreases promptly with increasing OA content from 0 to 30 mol % and then decreases slightly with further increasing OA content from 30 to 80 mol %. However, the PDI changes in a small range between 1.066 and 1.200. That is to say, the size distribution is always narrow, despite the variation of the OA/AN ratio. The respective smallest D_n and PDI of 97.6 nm and 1.066 appear at the OA/AN molar ratio of 80/20. It is surprising that the PDI down to 1.066 implies that the particles are nearly monodisperse. The size and shape of dry copolymer particles in ambient air were observed by AFM (Figure 2). The two types of particles both seem to be anomalistic ellipsoids, but their size is dependent on the OA/AN ratio. The OA/AN (50/50) copolymer particles have minor/major axis diameters of 85/150 nm, with an unsharp particle boundary, whereas the OA/AN(80/20) copolymer particles have smaller minor/major axis diameters of 75/110 nm with a relatively clear particle boundary.

TEM images of the copolymer particles with two OA/AN ratios are shown in Figure 3. It seems that the TEM morphology of the dispersion was spheric, ellipsoidal, fibrous, or clavellate nanostructure depending on the OA/AN ratio. Spheric and ellipsoidal particles with a number-average diameter of 34 nm and fibrous structures with a diameter of 12−20 nm were clearly and simultaneously observed in the OA/AN (50/50) copolymer system in Figure 3a−b. These results showed that there was no remarkable difference between the spheroidal shapes of the particles

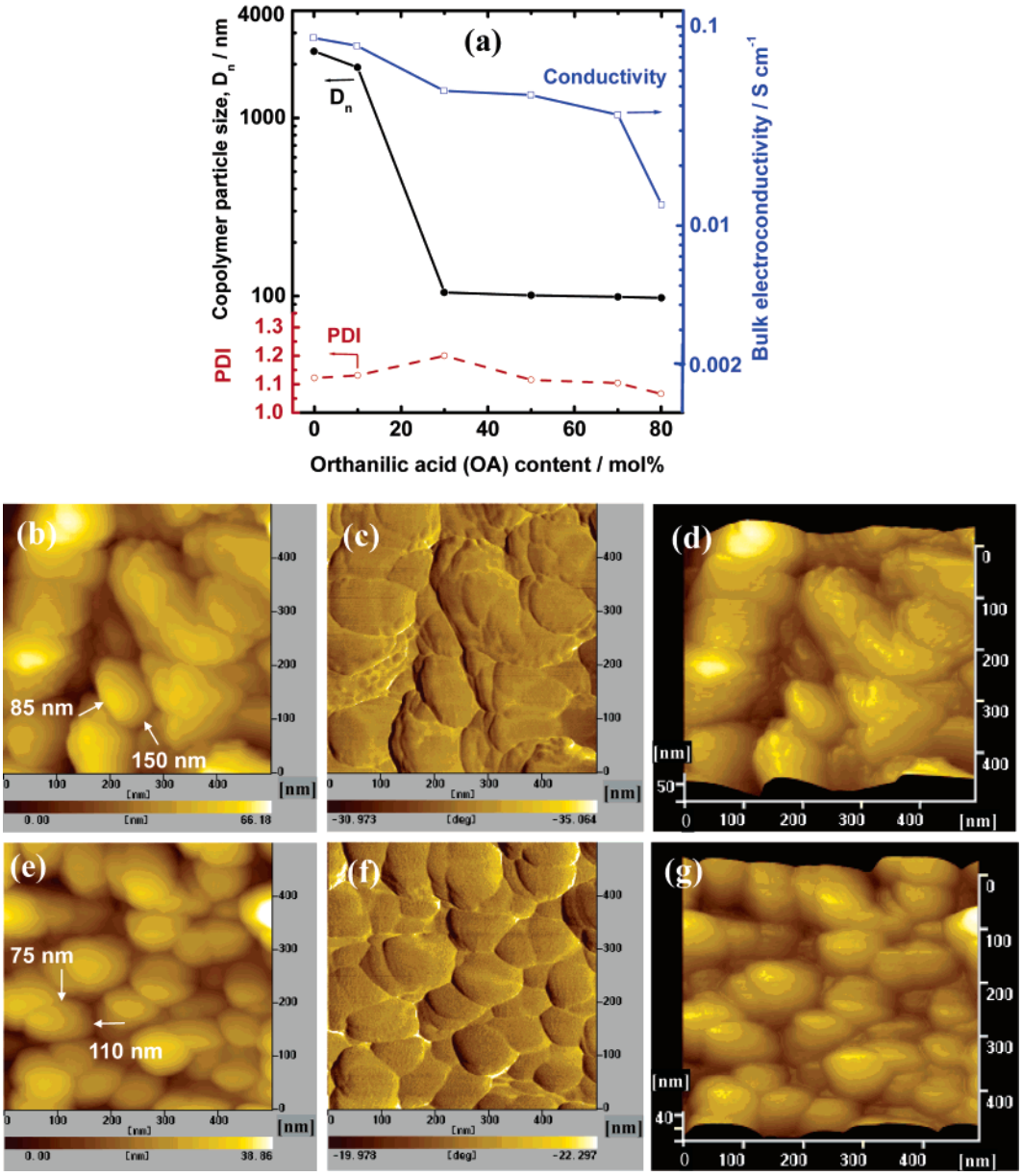

Figure 2. (a) Variation of number-average diameter (D_n), polydispersity index (PDI), and conductivity of OA/AN copolymer particles with orthanilic acid (OA) content under a fixed oxidant [$(NH_4)_2S_2O_8$]/monomer molar ratio of 0.5/1 in 1 M HCl for a polymerization time of 24 h at a polymerization temperature of 30 °C and a constant magnetostirring rate. The typical AFM topoimage (b), phase image (c), and three dimensional image (d) of OA/AN (50/50) copolymer dry particles on cover glass and the typical AFM topoimage (e), phase image (f), and three dimensional image (g) of OA/AN (80/20) copolymer dry particles on cover glass.

observed by TEM and AFM. Similar coexistence of granular and fibrous nanostructures was found in PAN polymerized at room temperature at an AN/HCl molar ratio of 1/0.5 in the presence of sodium dodecylbenzenesulfonate as a surfactant[20] and also in 2,5-disulfoaniline/AN copolymer synthesized in HCl aqueous solution without any external stabilizer in our laboratory. However, lots of clava with respective diameter and length of 15−38 and 200 nm, together with a small quantity of spheroidal particles with an average diameter of ∼28 nm, appeared in the OA/AN (80/20) copolymer system(see Figure 3c−d). The OA/AN-(80/20) copolymer particles change shape from ellipsoid, observed by AFM in an equilibrium ambient atmosphere, to barlike particles, by TEM in a high vacuum. This shape change implies a reorganization of chain conformation and sulfonic groups to accommodate or drive the shape change during further drying. Similar barlike nanostructured PAN obtained by emulsion polymerization has also been examined.[21] No fibrous nanostruture was clearly found in AFM images, since the AFM image is only a surface structure of the particles on the glass, but TEM is a totally bulk structure on the copper grid. Possibly, the nanostructured copolymers exhibit different dispersing states on the glass and copper grid. It could be speculated that very small nanospheroids floated at the top, but the relatively long nanoclavas sank to the bottom during the AFM observation. When the particles went from an extended to a conformationally collapsed state, this was accompanied by a significant increase in specific surface area. The functional nanoparticles with an anisotropic shape should be uncommon but very important for nanotechnological applications such as nanoactuators because the thermodynamically most stable form for polymer nano-

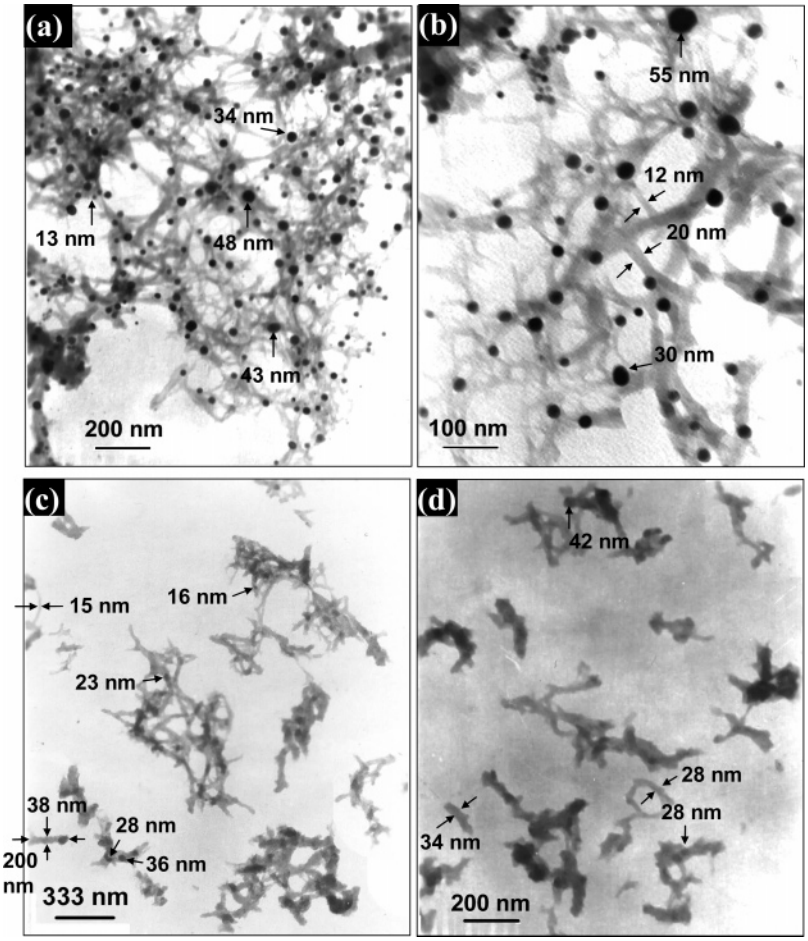

Figure 3. The TEM images of OA/AN (50/50) (a, b) and OA/AN (80/20) (c, d) copolymer dry particles obtained under an oxidant $[(NH_4)_2S_2O_8]$/monomer molar ratio of 1.5/1 [OA/AN (50/50)] and 0.5/1 [OA/AN (80/20)] in 1 M HCl for a polymerization time of 24 h at a polymerization temperature of 30 °C at a constant magnetostirring rate.

particles is spherical in shape as a result of minimizing surface energy.[22]

Note that a variation of the particle size with measurement methods from LPA, AFM, to TEM was found because of their different testing conditions. In addition, the collapsed particles observed by TEM are the smallest, but the water-swollen particles examined by LPA are the largest because of the contraction or shrinkage caused by an exclusion of water inside the particles containing many hydrophilic sulfonic groups during drying.[23] Fully extended sulfonic groups toward outside the particles also result in a larger hydrodynamic diameter. Similar instances have also been found for the particles of styrene/styrenesulfonate and AN/sulfodiphenylamine copolymers.[12,13] Anyway, the variation of the particle size with OA/AN ratio revealed by AFM and TEM is the same as that by LPA; i.e., the OA/AN(80/20) particle size evaluated by the three methods is always smaller than the OA/AN(50/50) particle size.

To find a favorable temperature for synthesizing the nanoparticles, the OA/AN (50/50) copolymerization was carried out at five temperatures ranging from 0 to 40 °C. The effect of polymerization temperature on the size of the copolymer particles is given in Figure 4. The D_n decreases when temperature is increased from 0 to 30 °C, but it remains unchanged in the temperature range of 30−40 °C, whereas the PDI changes in a narrow range from 1.115 and 1.296. In other words, the size polydispersity is always narrow regardless of polymerization temperature. The particles formed at 0 °C are the biggest (260 nm), partly due to the polymerizability of the OA, which is weaker with a monomer containing sulfonic side group with a great steric hindrance and electron-withdrawing effect than with the AN monomer, leading to fewer sulfonic groups on the polymer chain. Similar dependency of the particle size on the polymerization temperature has also been found for the AN/sulfodiphenylamine copolymers in our laboratory. In addition, AFM images also illustrate that the copolymer particles obtained at 40 °C (Figure 4) have a diameter that is similar to those obtained at 30 °C (Figure 2), but their shapes are slightly different. This could imply that the sulfonic group content on the copolymer chains formed at 30−40 °C is similar.

Figure 5 shows a complicated dependency of the particle size and its distribution of the OA/AN (50/50) copolymers on polymerization time. It seems that the particles of 64 nm at a polymerization time of 2 h are the smallest, then both D_n and PDI acutely increase to maximal values of 3600 nm and 1.213, respectively, at 10 h. After 10 h, the particle size reduces sharply and reaches the second smallest value of 70 nm at 48 h. A similar variation of the particle size with polymerization time has been observed for ethylaniline/sulfoanisidine copolymer particles.[19] The variation of the D_n and PDI with the polymerization time indicates a conglom-

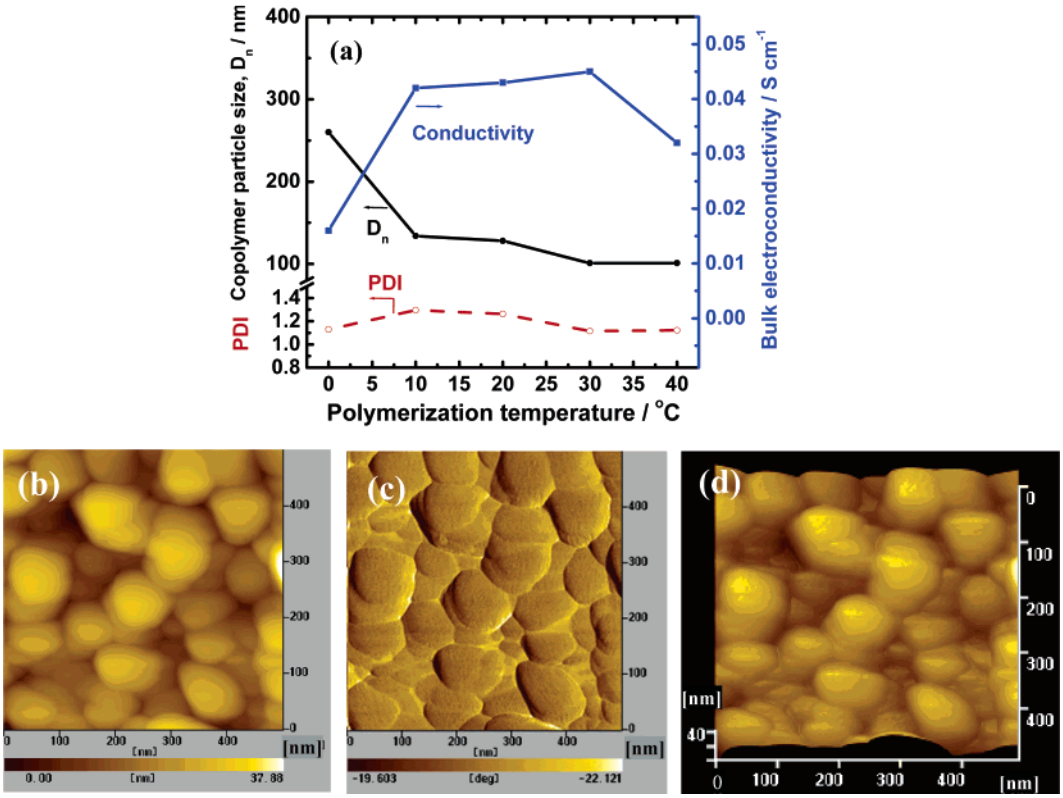

Figure 4. (a) Variation of number-average diameter (D_n), polydispersity index (PDI), and conductivity of OA/AN (50/50) copolymer particles with the polymerization temperature under a fixed oxidant [$(NH_4)_2S_2O_8$]/monomer molar ratio of 0.5/1 in 1 M HCl at a constant magnetostirring rate for a polymerization time of 24 h. The typical AFM topoimage (b), phase image (c), and three dimensional image (d) of OA/AN (50/50) copolymer dry particles on a cover glass for the copolymerization at a polymerization temperature of 40 °C

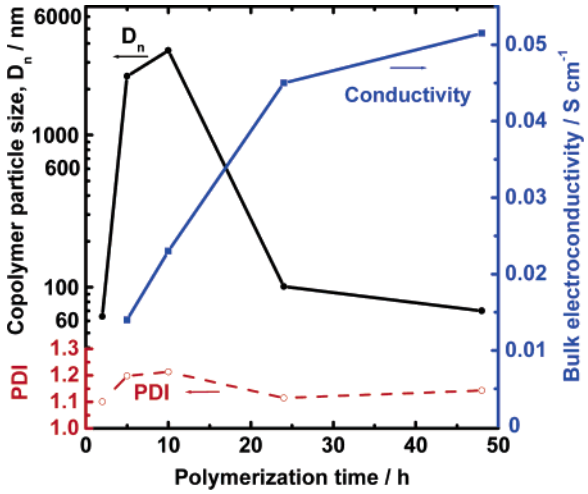

Figure 5. Variation of number-average diameter (D_n), polydispersity index (PDI), and conductivity of OA/AN (50/50) copolymer particles with polymerization time under a given oxidant [$(NH_4)_2S_2O_8$]/monomer molar ratio 0.5/1 and a polymerization temperature of 30 °C.

eration of small particles formed earlier and smash of large particles formed later during the OA/AN copolymerization. The conglomeration of small as-formed particles earlier should be a relatively spontaneous process, whereas the smash and uniformization of large particles formed later could be attributed to continual and vigorous magnetic stirring during the polymerization. Although a short polymerization time of ~2 h is of benefit to the formation of the very small particles, their productivity (Figure 1c) and properties are not good enough. Additionally, an extended time will enhance the cost of production. Therefore, the copolymerization time of 24 h favors synthesizing superfine particles. Similar optimal time for the formation of the AN/sulfodiphenylamine copolymer nanoparticles has also been observed in our laboratory.

From Figure 6, one can see that the optimal oxidant/monomer molar ratio is 1/1 for the formation of the smallest copolymer particles with the lowest PDI of 1.078. Lower oxidant content might result in an insufficient polymerization of the OA monomer with relatively lower reactivity, reducing the sulfonic group content in OA/AN copolymer and then static repulsion among the particles, finally leading to conglomeration of the particles to some extent. With increasing oxidant content, it seems that the particles become smaller because of higher sulfonic group content in OA/AN copolymer. Note that excessive oxidant is much more beneficial for the formation of the AN cation radicals, bringing on a higher concentration of the AN intermediates than that of the OA intermediates. Apparently, this is favorable for the formation of larger particles. AFM observation also verifies a similar variation of the particle size with the oxidant/comonomer ratio, as shown in Figure 6. A close observation of the AFM image in Figure 6b−e indicates that the copolymer particles of ellipsoidal shape with major/minor axes of 98/60 nm with an oxidant/monomer molar ratio 1/1 are different from those with an oxidant/monomer molar ratio 1.5/1(Figure 6f−h). In particular, when compared with Figures 5−6, these particles formed with an oxidant/monomer molar ratio of 1/1 have a clear borderline.

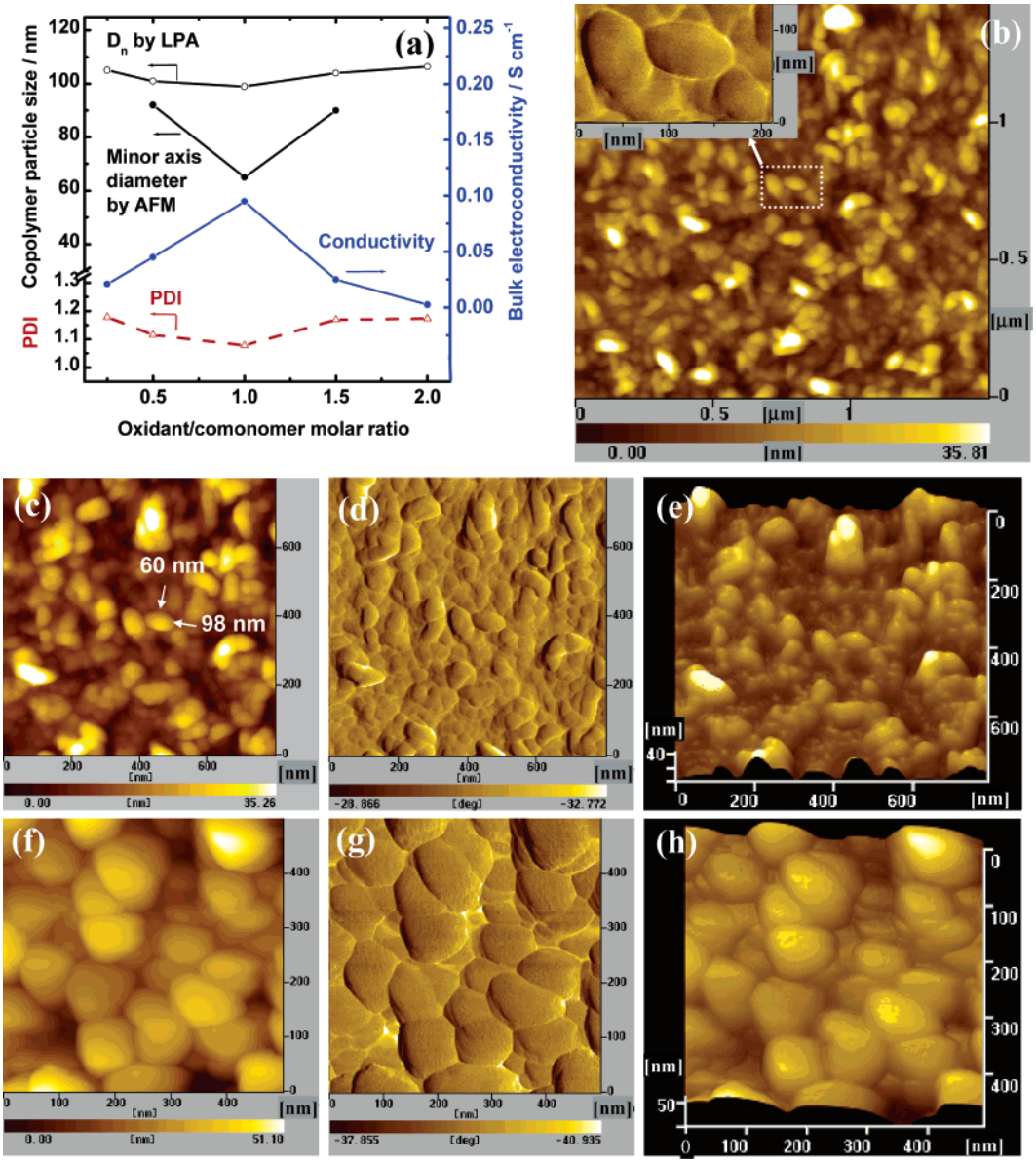

Figure 6. (a) Variation of size and conductivity of OA/AN (50/50) copolymer particles with oxidant [$(NH_4)_2S_2O_8$]/monomer molar ratio under polymerization conditions: polymerization time of 24 h, polymerization temperature of 30 °C. The AFM topoimage (b, c), phase image (b (inset), d) and three-dimension image (e) of OA/AN (50/50) copolymer dry particles prepared with an oxidant [$(NH_4)_2S_2O_8$]/monomer molar ratio of 1/1 and the AFM topoimage (f), phase image (g), and three-dimension image (h) of OA/AN (50/50) copolymer particles prepared with an oxidant [$(NH_4)_2S_2O_8$]/monomer molar ratio of 1.5/1.

Obviously, the effect of oxidant/monomer ratio on the shape of the OA/AN copolymer particles is significant.

In addition, it is found that the D_n and PDI of the OA/AN (30/70) copolymer particles with a fixed oxidant/monomer molar ratio 0.5/1 in 1 M HCl at 0−5 °C for 24 h decrease from 4.193 and 1.240 μm to 2.072 and 1.156 μm, respectively, after the ultrasonic treatment for half an hour. Particularly, the OA/AN (50/50) copolymer particles dramatically reduce their D_n and PDI from 2.677 and 1.250 μm to 260.4 and 1.129 nm, respectively, after the ultrasonic treatment. Apparently, ultrasonic dispersion is a simple and useful method to obtain smaller and even nanoparticles with a narrower size distribution.

It can be concluded that the presence of sulfonic groups on the OA monomers allows their copolymer particle size to be controlled by varying the OA/AN ratio and polymerization conditions because the sulfonic groups as an efficient internal stabilizer can produce static repulsion among the particles and further strongly stabilize the nanoparticles.

Properties of the OA/AN Copolymer Particles. 1. Solubility and Solvatochromism. All copolymers are soluble in NMP and concentrated H_2SO_4, with a high dielectric constant, but they are hardly soluble in DMF, THF, and $CHCl_3$, with low dielectric constant. With increasing OA content, the copolymers exhibit a steadily improved solubility in alkaline solutions. Furthermore, the copolymers with 70−80 mol % OA units are completely soluble in 0.1 M NaOH and NH_4OH but insoluble in THF and $CHCl_3$. With increasing OA unit content, the significantly enhanced solubility of the copolymers in alkaline solution but slightly reduced solubility in THF and $CHCl_3$ should be ascribed to the introduction of sulfonic groups into the copolymer. It can also be found that the color of the copolymers in H_2SO_4 and alkaline solutions changes significantly with OA content.

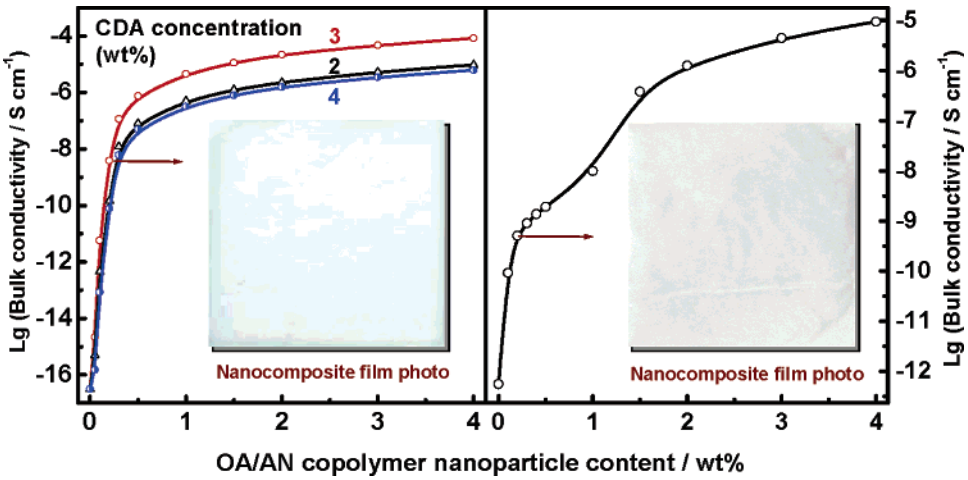

Figure 7. Bulk electrical conductivity vs OA/AN (50/50) copolymer nanoparticle content in CDA (left) and PVA (right) composite films. CDA concentration in glacial acetic acid for the film preparation: (△) 2, (○) 3, and (□) 4 wt %. Insets: Photographs of the nanocomposite films containing 0.2 wt % copolymer nanoparticles in 3 wt % CDA in glacial acetic acid (left) and in PVA (right).

Thus, it can be concluded that the variable solubility of the copolymers is principally due to a change in the molecular structure. The polymers obtained are not a simple admixture of two homopolymers but, rather, are genuine copolymers.

It is interesting that a color variation of OA/AN copolymer solution with the solvents is observed, that is, a novel solvatochromism. H_2SO_4 and alkaline solutions are red for the copolymers with OA content of no more than 30 mol % but blue for other copolymers, except for a green solution of OA/AN(80/20) copolymer in H_2SO_4. Noteworthily, all copolymer solution is green in DMSO and blue in NMP. These imply that their π-conjugated structure might change with OA/AN ratio and solvent used owing to different interaction between the copolymer chains and the solvent. In other words, the copolymer solvatochromism might be adjusted by choosing commoner ratio or solvent. Some copolymer solutions are blue of short wavelength,[23] suggesting short conjugated length, i.e., low electrical conductivity, as discussed below.

2. Bulk Electrical Conductivity. The bulk electrical conductivity of the OA/AN copolymers is summarized in Figures 2, 4−6, which varies in a small range from 2.4×10^{-3} to 9.5×10^{-2} S cm^{-1}, depending on the OA/AN ratio and synthesis conditions. The conductivity sharply decreases as the OA content increases from 0 to 30 mol % and 70 to 80 mol %. But at the OA content from 30 to 70 mol %, the conductivity slightly decreases from 4.9×10^{-2} to 3.9×10^{-2} S cm^{-1}. The reduced conductivity with increasing OA content is basically confirmed by the shortened wavelength of band II, due to the reduced conjugation length in distorted chains and the decrease in interchain charge transport, both of which are induced by the steric and electronic effect of bulky sulfonic groups. Moreover, the intrachain and interchain electrostatic interactions between $-SO_3^-$ groups and main-chain cationic nitrogen atoms would also decrease the conductivity. Distinctly, the OA/AN(50/50) copolymer nanoparticles possess a well-balanced combination of high conductivity, small size, and a narrow size distribution that is very desirable for their application.

Figure 4 shows the conductivity of OA/AN(50/50) copolymers formed in a polymerization temperature range from 0 to 40 °C. It seems that the maximal conductivity appears at 30 °C, implying that the copolymers formed at 30 °C consist of the longest conjugating structure because low temperature is not favorable for the chain propagation of OA monomer, whereas high temperature is not favorable for the chain propagation of AN monomer. The variation of the conductivity of the OA/AN(50/50) copolymers with polymerization time is summarized in Figure 5. The conductivity first rises significantly with prolonged polymerization time and then reaches a plateau, suggesting that the chain propagation of the copolymers is very remarkable before 24 h.

Figure 6 illustrates that the OA/AN copolymers show a maximal conductivity of about 9.5×10^{-2} S cm^{-1} at an oxidant/comonomer molar ratio of 1/1, possibly due to the highest self-doping level from $-SO_3H$. That is to say, the highest $-SO_3H$ content results in the formation of the nanoparticles with the smallest size and PDI but the highest conductivity. In a word, the OA/AN(50/50) copolymer nanoparticles polymerized at 30 °C for 24 h with the oxidant/comonomer molar ratio of 1/1 have the optimal combination of high conductivity, high yield, small size, and narrow size distribution. Uniquely, the conductivity substantially stays unchanged, even after treatment with alkaline solutions,[24] suggesting a stable and high self-doping structure from versatile $-SO_3H$ groups.[8] As a result, the nanoparticles with a stable conductivity and novel ellipsoid/rod shape are very favorable to be simply and directly applied in nanocomposite materials.

Electroconducting Nanocomposite Films. It is the attractive qualities of environmental stability, satisfactory conductivity, and ease of chemical synthesis that make OA/AN copolymer nanoparticles an excellent choice to blend with conventional polymers. Therefore, the nanoparticles have become the favorite choice for the fabrication of the conductive composites simply because the nanoparticles are capable of dispersing facilely and uniformly in the various polymer solutions and exhibit a good conductivity under multitudinous environments.

The variation of electrical conductivity of the nanocomposite films with the nanoparticle loading is shown in

Scheme 1. Chemical Oxidative Copolymerization of Orthanilic Acid and Aniline

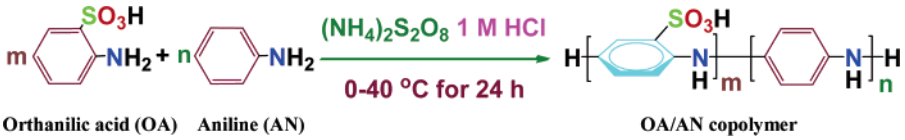

Figure 7. It is observed that the nanocomposite films exhibit reasonably high conductivity, even with low nanoparticle loading. Consistent with the percolation theory, these data indicate percolation threshold and critical exponent values of 0.18 wt % and 1.9, respectively, for the CDA system. This percolation threshold is relatively low, and the exponent is similar to that for a three-dimensional conducting nanocomposite film of PAN nanoparticles and poly(vinyl chloride).[25] Three series of nanocomposite films with the same nanoparticle content have been studied by changing CDA concentrations in acetic acid. As shown in Figure 7a, it seems that the CDA concentration has an influence on the conductivity. An upmost conductivity appears at the CDA concentration of 3 wt %; however, the critical exponent of nanocomposite films is not dependent on the concentration of CDA in acetic acid.

In Figure 7b, PVA as the matrix of the composite film appears to be an interesting case that has double percolation thresholds: 0.07 and 0.91 wt %, corresponding to the conductivities of 10^{-10} and 10^{-8} S cm^{-1}. In addition, the critical exponent of the nanocomposite films is 1.1 and 1.9, and the first critical exponent is much smaller than the value predicted by the universal law (2.0) that can be attributed to the formation of an insular conducting zone rather than a conducting network by the nanoparticles.[25]

The insets in Figure 7 show the photographs of the nanocomposite films containing the same 0.2 wt % OA/AN copolymer nanoparticles in CDA and PVA, which differ significantly. CDA-based nanocomposite film exhibits a smooth surface and light color, in which the nanoparticles tend to aggregate on the boundary to some extent, whereas PVA-based nanocomposite film has very uniform nanoparticle dispersion and high mechanical property, enduring a folding of more than 100 times. Apparently, the PVA-based nanofilm exhibits better flexibility and uniform dispersity, whereas the CDA-based nanofilm has higher transparency and conductivity. All these suggest that the matrix polymer also plays an important role in nanocomposite films.

Conclusions

Libraries of novel OA/AN copolymer nanoparticles with an intrinsically narrow size distribution have been triumphantly synthesized by oxidative copolymerization. AN could be a highly efficient activator for OA polymerization, simply conquering a difficulty of the oxidative homopolymerization of OA monomer. Copolymerization yield, as well as the macromolecular structure, particle size, and properties of the copolymers, all significantly depend on the OA/AN ratio because of oxidative polymerizability that is much weaker in OA than in AN. Moreover, the reaction conditions, such as the temperature and time of polymerization and oxidant/monomer ratio have a remarkable influence on the particle size/shape and electrical conductivity. The OA/AN copolymer nanoparticles are a mixture of spheroid (28−34 nm), fibril (12−20 nm), or bar (15−38 nm), whose bulk conductivity is up to 9.5×10^{-2} S cm^{-1}. The polydispersity index of the particle sizes always stays at a small value between 1.066 and 1.296. A nonmonotonic variation of the UV−vis spectra of the copolymers with OA/AN ratio suggests that the polymers formed are actual copolymers. The OA/AN-(50/50) copolymer nanoparticles formed at oxidant/comonomer molar ratio of 1/1 as well as the polymerization temperature and time of 30 °C and 24 h, respectively, have the optimal combination of high yield, high conductivity, small size, and narrow size distribution. Nanocomposite films of the nanoparticles and conventional polymers exhibit very low percolation threshold and transparency and flexibility, which endow them with a widely potential application as antistatic materials and advanced packaging films. Although the vastly simplified concept of the direct preparation of conducting nanoparticles featuring a good self-stability and pure composition was successfully demonstrated with only an OA comonomer, the oxidative precipitation copolymerization of other sulfonic AN monomers with AN or other aromatic amines incorporating a wide variety of functionalities is conceivable. Extension of our technique to these new monomers will allow for the preparation of nanoparticles tailored for specific versatilities, such as variable electroconductivity, high metal-ion adsorptivity, and colorful electrochromism.

Experimental Section

Orthanilic acid (OA), aniline (AN), ammonium persulfate, cellulose diacetate (CDA), poly(vinyl alcohol) (PVA), sulfuric acid, hydrochloric acid, *N*-methylpyrrolidone (NMP), dimethyl formamide (DMF), dimethyl sulfoxide (DMSO), tetrahydrofuran (THF), and chloroform ($CHCl_3$) were commercially obtained and used as received.

The chemically oxidative precipitation polymerization for the synthesis of the OA/AN copolymer nanoparticles was carried out with ammonium persulfate as an oxidant in HCl aqueous solution.[13,22] A typical procedure is as follows: 0.87 g (5 mmol) of OA and 0.47 g (5 mmol) of AN were dissolved in 100 mL of a 1.0 M HCl solution and stirred vigorously at 30 °C for 0.5 h. An oxidant solution of 1.14 g (5 mmol) ammonium persulfate in 50 mL of 1.0 M HCl was added dropwise into the monomer solution at a rate of 1 drop (∼60 μL) every 3 s. This mixture was vigorously magnetostirred for 24 h at 30 °C, and the dark precipitate obtained was filtered and washed with water until the filtrate was colorless. The fine powders were left to dry in ambient air for 1 week. The nominal copolymerization and molecular structure of the final copolymer are described in Scheme 1.

Two series of nanocomposite films were prepared by a cast method of a CDA or PVA solution containing the OA/AN copolymer nanoparticles. For the nanoparticle/CDA

films, 2, 3, and 4 wt % CDA solutions in glacial acetic acid were mixed with appropriate amounts of the nanoparticles and then ultrasonically treated for 3 h. The ultrasonic solution was cast onto a glass substrate and dried at an elevated temperature. The nanoparticle/PVA films were prepared by a similar procedure, except that the water was used as a solvent and poly(tetrafluoroethylene) was used as a substrate.

The open-circuit potential (OCP) of the polymerization solution was in situ measured by an OCP technique using a saturated calomel electrode (SCE) as a reference electrode and a platinum foil as a working electrode. IR spectra of the polymer/KBr pellets were recorded on a Nicolet Magna 550 Fourier transform infrared (FTIR) spectrometer at 2 cm^{-1} resolution. UV−vis spectra were obtained on a Perkin-Elmer Lambda-35 spectrophotometer in a wavelength range of 190−900 nm at a scanning rate of 480 nm/min, slit of 2.0 nm, and wavelength correctness of ±0.3 nm at a polymer concentration of 0.01 mg/mL NMP. The size and its distribution of the polymer particles in water were analyzed by a Beckman Coulter LS 230 Laser Diffraction Particle-Size Analyzer. The atomic force microscopy (AFM) images were taken in a tapping mode by using an SPA-300HV AFM system, Seiko SII Instruments, Japan, with a resolution of 0.2 nm in the *XY* direction and 0.01 nm in the *Z* direction. The scanning tip was a silicon microcantilever (SI-DF20, Seiko Instruments, spring constant = 12 N/m, average resonance frequency = 135 kHz). The AFM sample was prepared by dropping the dilute aqueous solution of the freshly synthesized particles on a cover glass and then drying for 1 h at 30 °C. The sample for a Hitachi model H600 transmission electron microscopy (TEM) was prepared by dipping a copper grid into the suspension of the particles that had been stored in water for about 1 year. The solubility of dry particles was evaluated as follows: Polymer powders of 10 mg were added into the solvent of 1 mL and dispersed thoroughly. After the mixture was swayed continuously for 24 h at room temperature, the solubility was characterized semiquantitatively. Since the dried copolymer particles are blackish green, a dark solution color but no solid residues in the solution suggests that the polymer is soluble. A dark solution color but a few solid residues in the solution indicates mainly soluble polymer. An obvious solution color but moderate solid residues in the solution signifies that the polymer is partly soluble. Light solution color but more solid residues in the solution implies that the polymer is slightly soluble. Colorless solution but all solid residues was observed in the solution, suggesting insolubility. Bulk electrical conductivity of as-formed polymer salts was measured by a two-disk method at 15 °C.

Acknowledgment. The project was supported by National Natural Science Foundation of China (20274030) and the Shanghai Key Laboratory of Molecular Catalysis and Innovative Materials, Fudan University. We thank Prof. Dr. Dong-Yuan Zhao, He-Yong He, Guo-Xin Jin, and Ming-Fei Zhou in Fudan University for their valuable help.

Supporting Information Available. The solubility, solution color, the open-circuit potential of copolymerization solution and IR and UV−vis spectra are available as Supporting Information. This material is available free of charge via the Internet at http://pubs.acs.org.

References and Notes

(1) Varela, H.; Maranhao, S. L. de A.; Mello, R. M. Q.; Ticianelli, E. A.; Torresi; R. M. *Synth. Met.* **2001**, *122*, 321−327.
(2) Janata, J.; Josowicz, M. *Nat. Mater.* **2003**, *2*, 19−24.
(3) Yu, X.; Sotzing, G. A.; Papadimitrakopoulos, F.; Rusling, J. F. *Anal. Chem.* **2003**, *75*, 4565−4571.
(4) Li, C. M.; Mu, S. L. *Synth. Met.* **2004**, *144*, 143−149.
(5) Wang, Y. Z.; Sun, R. G.; Meghdadi, F.; Rusling, J. F. *Synth. Met.* **1999**, *102*, 889−892.
(6) Koul, S.; Dhawan, S. K.; Chandra, R. *Synth. Met.* **2001**, *124*, 295−299.
(7) Yue, J.; Wang, Z. H.; Cromack, K. R.; Epstein, A. J.; MacDiarmid, A. G. *J. Am. Chem. Soc.* **1991**, *113*, 2665−2671.
(8) Malinauskas, A. *J. Power Source* **2004**, *126*, 214−220.
(9) Barbero, C.; Salavagione, H. J.; Acevedo, D. F.; Grumelli, D. E.; Garay, F.; Planes, G. A.; Morales, G. M.; Miras, M. C. *Electrochim. Acta* **2004**, *49*, 3671−3686.
(10) Sanghvi, A. B.; Miller, K. P.-H.; Belcher, A. M.; Schmidt C. E. *Nat. Mater.* **2005**, *4*, 496−502.
(11) Mav, I.; Zigon, M.; Sebenik, A.; Vohlidal, J. *J. Polym. Sci., Part A: Polym. Chem.* **2000**, *38*, 3390−3398.
(12) Sunkara, H. B.; Jethmalani, J. M.; Ford, W. *J. Polym. Sci., Part A: Polym. Chem.* **1994**, *32*, 1431−1435.
(13) Li, X. G.; Zhou, H. J.; Huang, M. R.; Zhu, M. F.; Chen, Y. M. *J. Polym. Sci., Part A: Polym. Chem.* **2004**, *42*, 3380−3394. (b) Li, X. G.; Lü, Q. F.; Huang, M. R. *Chem.−Eur. J.* **2006**, *12*, 1349−1359.
(14) Chattopadhyay, D.; Banerjee, S.; Chakravorty, D.; Mandal, B. M. *Langmuir* **1998**, *14*, 1544−1547.
(15) Moulton, S. E.; Innis, P. C.; Kane-Maguire, L. A. P.; Ngamna, O.; Wallace, G. G. *Curr. Appl. Phys.* **2004**, *4*, 402−406.
(16) Fan, J. H.; Wan, M. X.; Zhu, D. B. *Chin. J. Polym. Sci.* **1999**, *17*, 165−170.
(17) Li, X. G.; Duan, W.; Huang, M. R.; Yang, Y. L.; Zhao, D. Y. *Polymer* **2003**, *44*, 6273−6285.
(18) Albuquerque, J. E.; Mattoso, L. H. C.; Balogh, D. T.; Faria, R. M.; Masters, J. G.; MacDiarmid, A. G. *Synth. Met.* **2000**, *113*, 19−22.
(19) Li, X. G.; Huang, M. R.; Feng, W.; Zhu, M. F.; Chen, Y. M. *Polymer* **2004**, *45*, 101−115.
(20) Zhang, Z.; Wei, Z.; Wan, M. *Macromolecules* **2002**, *35*, 5937−5942
(21) Yu, L.; Lee, J.-II.; Shin, K. W.; Park, C. E.; Holze, R. *J. Appl. Polym. Sci.* **2003**, *88*, 1550−1555.
(22) Yang, Z.; Huck, W. T. S.; Clarke, S. M.; Tajbakhsh, A. R.; Terentjev, E. M. *Nat. Mater.* **2005**, *4*, 486−490.
(23) Li, X. G.; Hua, Y. M.; Huang, M. R. *Chem.−Eur. J.* **2005**, *11*, 4247−4256.
(24) Wei, X. L.; Wang, Y. Z.; Long, S. M.; Bobeczko, C.; Epstein, A. J. *J. Am. Chem. Soc.* **1996**, *118*, 2545−2555.
(25) Banerjee, P.; Mandal, B. M. *Synth. Met.* **1995**, *74*, 257−261.

CC050126Y